Medicine in Novel Technology and Devices 18 (2023) 100219

Contents lists available at ScienceDirect

Medicine in Novel Technology and Devices

journal homepage: www.journals.elsevier.com/medicine-in-novel-technology-and-devices/

Review Article

The sound of blood: photoacoustic imaging in blood analysis

Mitchell Veverka [a], Luca Menozzi [b], Junjie Yao [b,*]

[a] Duke University Hospital System, United States
[b] Duke University, United States

ARTICLE INFO

Keywords:
Photoacoustic imaging
Blood analysis
Pathogen detection
Analytes
Photoacoustic flow cytometry
Novel diagnostic technique

ABSTRACT

Blood analysis is a ubiquitous and critical aspect of modern medicine. Analyzing blood samples requires invasive techniques, various testing systems, and samples are limited to relatively small volumes. Photoacoustic imaging (PAI) is a novel imaging modality that utilizes non-ionizing energy that shows promise as an alternative to current methods. This paper seeks to review current applications of PAI in blood analysis for clinical use. Furthermore, we discuss obstacles to implementation and future directions to overcome these challenges. Firstly, we discuss three applications to cellular analysis of blood: sickle cell, bacteria, and circulating tumor cell detection. We then discuss applications to the analysis of blood plasma, including glucose detection and anticoagulation quantification. As such, we hope this article will serve as inspiration for PAI's potential application in blood analysis and prompt further studies to ultimately implement PAI into clinical practice.

1. Introduction

The human body contains up to 10% blood by weight [1]. Blood is a complex fluid composed of water, cells, metabolites, electrolytes, proteins, and hormones. Furthermore, it permeates, affects, and is affected by every organ of the body. Its functions range broadly from transportation of catabolic fuel and removal of metabolic waste to healing and microbial defense. Thus, testing of this omnipresent fluid can provide vast information regarding the body's physiological and pathophysiologic status.

Obtaining and testing samples of blood provides invaluable information; however, it comes with drawbacks. Blood sampling requires invasive procedures which can be uncomfortable and result in adverse events [2]. In preclinical settings, test subject size (e.g. mouse models) can make blood collection difficult [3]. In addition, laboratory analysis of blood components involves chemical reactions and/or enzyme assays which can result in differences from in-vivo environments [4–6]. Furthermore, testing for specific blood components can require separate, complex, and expensive equipment [7]. Finally, the small sample volume used in blood tests make it challenging to detect rare events such as circulating tumor cells in early metastasis [8].

Early technological advancements have transitioned a few specific blood measurements to non-invasive methods but are rather limited in their sensitivity [9–11]. Beyond these few cases, many desired blood measurements remain inestimable to existing biosensors. Photoacoustic imaging (PAI) is a developing technology that may play a role in future applications of blood analysis in clinical and preclinical realms. Due to its seamless combination of optical contrast and acoustic detection, this technology may provide methods of non-invasive blood analysis that current methods cannot. Using its deep-imaging properties beyond the skin surface, this technology demonstrates promise in reducing patient/subject harm and improving in-vivo analysis.

PAI operates via the photoacoustic effect. A molecule absorbs an electromagnetic wave in the form of a laser pulse, resulting in a temperature rise. This temperature rise induces a thermoelastic expansion of the molecule of interest causing ultrasonic waves to propagate outwards [12]. The waves are detected by an ultrasound transducer and reconstructed into an image that maps the original optical energy deposition, i.e. optical absorption. These PA waves can originate from both endogenous (particularly hemoglobin) and exogenous contrast agents such as nanoparticles, making for a wide range of imaging targets [13,14]. Furthermore, PAI benefits from the tunability of the image contrast through the selection of excitation laser wavelength, allowing for many molecules to be independently imaged using the same imaging system [15].

Due to the unique combination of both optics and acoustics, PAI has inherited the advantages of pure optical and ultrasound imaging systems. Similar to optical imaging systems such as optical coherence tomography and confocal microscopy, PAI systems can achieve high-resolution, high frame-rate, and strong contrast and sensitivity, all using non-ionizing

* Corresponding author.
E-mail addresses: mitchell.veverka@duke.edu (M. Veverka), luca.menozzi@duke.edu (L. Menozzi), junjie.yao@duke.edu (J. Yao).

https://doi.org/10.1016/j.medntd.2023.100219
Received 29 November 2022; Received in revised form 25 February 2023; Accepted 26 February 2023

Table 1
Summary of example optical imaging methods with their lateral resolution and depth limitations. Photoacoustic Microscopy (PAM).

Imaging Modality	Resolution (Lateral)	Depth
Confocal Microscopy	180 nm [18]	100 μm [19]
Optical Coherence Tomography	~5 μm [20]	3 mm [21]
Raman Scattering Microscopy	300 nm – 2 μm [22]	20 μm–100 μm [23]
Optical Resolution PAM	2.6 μm [24]	1.2 mm [24]
Acoustic Resolution PAM	45 – 590 μm [25]	3 – 10.3 mm [25]
Photoacoustic Tomography (dependent on array used)	100 – 720 μm [26]	10 – 70 mm [26]

radiation [16]. Moreover, due to weak acoustic attenuation of the biological tissues, the imaging depth of PAI is usually greater than pure optical imaging systems [17]. Compared with pure ultrasound imaging, PAI has inherent functional and molecular sensitivity to the tissue status based on the rich optical absorption contrast. These properties make PAI a versatile technology with a wide range of preclinical and clinical applications. (See Table 1).

The specific performance of a PAI system depends on the system's optical and acoustic configurations. Although there are more variations of imaging modalities than listed here, this paper will provide a brief overview of three broad groups of PAI systems: optical resolution photoacoustic microscopy (OR-PAM), acoustic resolution photoacoustic microscopy (AR-PAM) and photoacoustic computed tomography (PACT). As seen in Fig. 1, each modality relies on the photoacoustic effect but varies in the design based upon the desired imaging depth and spatial resolution. The readers are encouraged to refer to papers regarding the specific methods with more detailed descriptions [16,25,27–30].

OR-PAM provides the best imaging resolution and relies mostly on tight focusing of ballistic photons. Images by OR-PAM are limited to approximately 1 mm of depth (the optical diffusion limit in soft tissues), but can achieve an axial resolution of tens of microns and a lateral resolution of several microns or even sub-microns [29]. This imaging modality serves well for histology of tissue slices and can provide single-cell or organelle-level information

AR-PAM uses a wide-field optical excitation and relies on diffusive photons, which allows for greater penetration depths. Although the penetration depth is increased, the resolution becomes limited by the focused detection of high-frequency acoustic signals. Therefore, the resolution of AR-PAM systems depends on the focused transducer central-frequency, bandwidth, and focusing geometry [25]. For example, AR-PAM can use a 5 MHz transducer to image at a depth of 10.3 mm with a lateral resolution of 590 μm. Conversely, with a transducer at 40 MHz, AR-PAM is able to obtain a lateral resolution of 85 μm at a depth of 3.1 mm. Periyasamy et al. used a 30 MHz transducer and achieved a 57 μm axial resolution at a depth of 11 mm, whereas Moothanchery et al. used a 75 MHz transducer producing an axial resolution of 53 μm at a depth of 1.8 mm [27,32].These studies provide examples of the wide range of resolutions AR-PAM can produce depending on the acoustic configurations.

PACT utilizes wide-field optical excitation in the diffusive regime, low-frequency array transducers, and inverse reconstruction algorithms to provide a tomographic image [28]. PACT systems can provide rapid 2D or 3D imaging with resolutions at the sub-millimeter level. A wide range of ultrasound transducer arrays have been explored by PACT for signal detection including linear arrays, ring arrays, and 2D planar or hemispherical arrays [33–35]. These imaging systems have various spatial resolution and imaging depths, which are jointly determined by the acoustic detection geometry and frequency. Because PACT often utilizes array transducers for parallel signal detection, PACT can acquire an image much faster than traditional PAM [36].

The optimal selection of PAI system subtype depends on the characteristics of the targets to be imaged. While depth and resolution are important factors to be considered, the target must also either have an endogenous chromophore or be labeled with an exogenous chromophore. Endogenous chromophores such as hemoglobin have an intrinsic PA contrast, providing label-free vascular imaging [37,38]. Conversely, some targets may require labeling with nanoparticles and/or organic dyes to produce contrast of the desired target [13,14].

As will be demonstrated throughout this paper, PACT and AR-PAM play a particularly important role in in-vivo blood analysis due to their depth advantage over traditional optical imaging systems that are usually limited to superficial depths of analysis (<2 mm) [39]. Skin anatomy reveals capillary vessel depth resides around 1–4 mm, whereas venules and arterioles lie below this depth, which are out of reach for optical imaging systems. Although capillaries play a significant role in certain pathophysiology, critical information may be lost at the venule/arteriole level. Photoacoustic imaging provides a solution to this limitation through utilization of diffusive photons and acoustic signals.

Technical innovations in photoacoustic imaging continue to improve resolution, decrease acquisition time, and produce novel molecular contrasts, opening new possibilities for biomedical applications [40]. Its non-ionizing, acoustic and optical capabilities make it well poised for use in in-vivo settings.

While not exhaustive, this paper seeks to provide a review of current techniques applicable to blood analysis using PAI. We have organized this paper to parallel that of blood composition as seen in Fig. 2. First, we provide examples of applications to the cellular component of blood including: red blood cell pathology, bacterial pathogen detection and malignant cell identification. We then transition to examining applications to the acellular (plasma) component including: pharmacologic

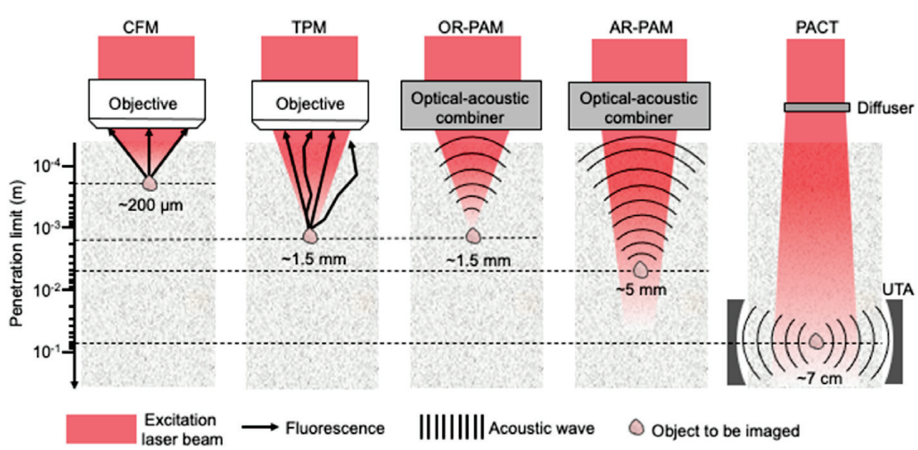

Fig. 1. Overview of CFM (confocal microscopy), TFM (two-photon microscopy), OR-PAM, AR-PAM, and PACT, produced by Wang and Yao [31].

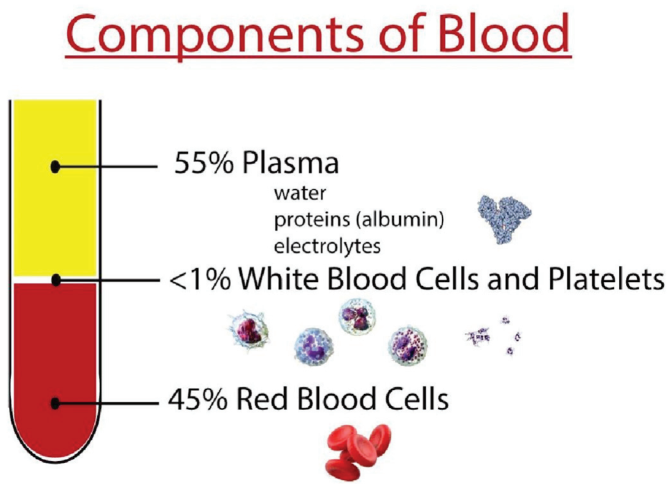

Fig. 2. Components of whole blood. Plasma is predominantly composed of water but contains many other active components. In addition to the listed components above, plasma contains diffused gasses, hormones, metabolites, waste products among others.

analysis and electrolyte quantification. PAI's potential is vast and accordingly we hope this paper helps establish the significance of PAI in blood analysis and provide inspiration for future work in developing this technology.

2. Applications to cellular components in blood analysis

Traditional hematological histopathology involves blood smear analysis with the use of light microscopy and hematoxylin and eosin (H&E) staining [41]. Although historically useful, traditional methods are limited in throughput and the staining can affect molecular processes [42]. Photoacoustic imaging shows promise for alternative methods for observing cellular components of the blood both in-vitro and in-vivo. This section of the paper reviews the current methods, advantages, and limitations regarding PAI's application to imaging several cellular components of blood associated with sickle cell disease, pathogen detection, and circulating tumor cells.

2.1. Sickle cell disease

Sickle cell disease is a pathology of red blood cells (RBC), whereby a mutation in hemoglobin (Hb) results in deformation of cells in the form of a sickle. This deformation is thus known as sickling of the cells. This sickling is followed by two important pathophysiologic changes. First, a decrease in oxygen saturation of Hb leading to decreased oxygen delivery to the tissues [43]. Second, a clustering of cells impeding blood flow and thus tissue perfusion [44]. The clinical sequelae of sickle crises vary, but early diagnosis is critical for the prevention and possible reversal of this process.

One common complication of sickle cell disease is a pain crisis. These pain crises are a result of micro vaso-occlusions, the etiology of which varies. Currently, there are no objective detection methods of these vaso-occlusions. Thus, diagnosis is made on the basis of subjective patient information which makes episodes difficult to predict and treat [45]. Without objective evidence physicians can easily under- or over-treat symptoms [46]. Objective detection of vaso-occlusions could improve diagnosis and thus improve treatment regimens.

Photoacoustic imaging may provide a method for this detection. Initial studies utilized PAI to demonstrate the ability to detect erythrocyte changes using photoacoustic flow cytometry (PAFC). Biswas et al. determined differences in cell shape and size with in-vitro methods while Strohm et al. demonstrated the differences in RBC orientation effects on PA signals [47,48]. Fig. 3 demonstrates an example image using PAM of normal red blood cells (nRBCs) and sickled red blood cells (sRBCs). These studies were then validated by theoretical analyses providing mathematical foundations to understanding the PA signal changes, quantifying cell orientation and shape [47].

Due to the structural changes between sickle cell hemoglobin (HbSS) and natural Hb hemoglobin, Cai et al. demonstrated PA signal differences between RBCs (prior to sickling) containing these two Hb states (Hb and HbSS) [49]. They also showed differences in PA signals between cells that had sickled and those that contained HbSS but had not yet sickled. With this information, clinicians could detect an acute change in the ratio of sickled cells present within the body. Although a rapid change in the percentage of sickled cells may result in an acute pain crisis, further studies are needed for verification. While sickling percentage contributes to vaso-occlusions, measurement RBC movement through vessels may provide another method to quantifying vaso-occlusive crises. Galanzha et al. monitored various rheology parameters within microvascular using PAI. Their team was able to identify aggregations of RBCs and flow rate of RBC movement through microvasculature [50]. Ultimately, these observations may provide objective data thought to contribute to acute pain crises

Importantly, many of these studies also provided in-vivo demonstration for detecting the aforementioned information [48–50]. As previously mentioned, healthcare providers currently rely on subjective data to determine acute pain crises. PAI succeeds in providing an objective

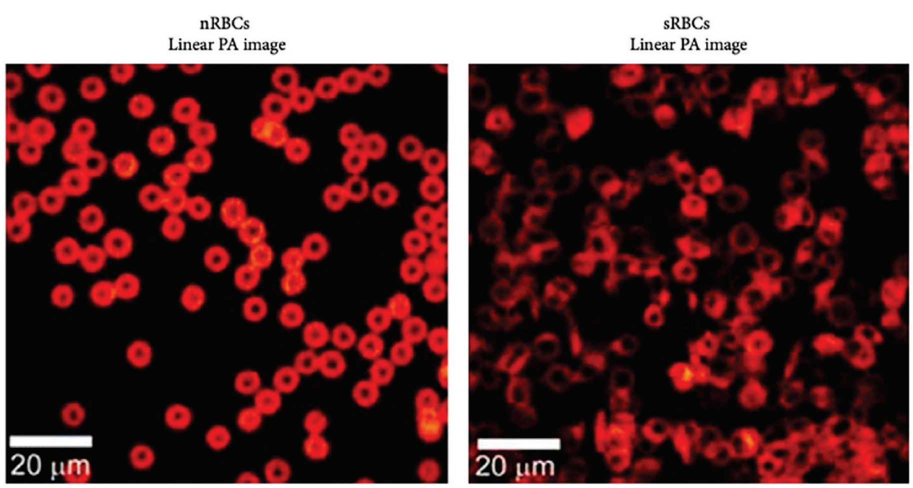

Fig. 3. Photoacoustic images of normal RBCs (nRBC, left image) and photoacoustic images of sickled RBCs (sRBC, right image) produced by Cai et al. [49].

data source which can be acquired non-invasively. With the identification of an acute change in the quantity of sickle cells, scale of aggregation, and change in microvascular flow, physicians could implement more optimal pain treatment in sickle cell patients. Further pilot studies are needed to demonstrate the effectiveness of PAI in assessing the relationship of hemorheological changes during sickle cell pain crises.

2.2. Pathogen detection in the blood

More than 670 million communicable diseases occur each year and are the eighth leading cause of death worldwide [51–53]. A large portion of these diseases have treatments that are both effective and relatively low-cost, but they rely upon early and accurate diagnosis. There are two notable areas of communicable diseases in which PAI may provide clinical benefit with early diagnosis and treatment evaluation: malaria and bacteremia.

2.2.1. Malaria

Malaria is a parasite that is reliant on RBCs as a host. The parasite is transmitted via mosquito and is endemic to primarily tropical and subtropical regions of the world. The disease affects up to 230 million patients per year, 400,000 of which result in death [54]. Early diagnosis and complete disappearance of the infection are key to treatment [55]. Current diagnosis involves invasive blood sampling and high-resolution microscopy with an experienced diagnostician, which is not always available in the regions most affected by the disease. There have been many attempts at improving the diagnosis of malaria, but none have been entirely successful in reducing complexity and optimizing diagnosis rate [56].

PAI provides a possible alternative with earlier detection rates and better ease-of-use. Malaria starts as a sporozoite entering the bloodstream via mosquito bite. These sporozoites infect hepatocytes and mature into merozoites, which in turn infect red blood cells. The parasite cycles between infecting red blood cells, reproducing, rupturing red blood cells and thus releasing and infecting other cells [57]. During its merozoite stage, the parasite breaks down hemoglobin producing a byproduct known as hemozoin [58].

Initial studies with PAI demonstrated hemozoin produces a strong PA signal, enabling its use as a surrogate marker for the presence of malaria [56,59]. Traditional optical of thick blood film is the gold standard for detection of malarial parasites but has a detection limit of approximately 50 parasites/microliter and only a sensitivity of around 85% [60,61]. Conversely, more advanced methods have reported a higher sensitivity, but detection limits have not greatly improved [61]. PA flow cytometry (PAFC) is a method by which cells move in a single file through a pulsed laser. Fig. 4 pictorially demonstrates in-vivo PAFC. Each cell that passes by a photoacoustic laser and sensor, which produces a corresponding PA signal. Each of these signals is analyzed to determine if the cell contains hemozoin and thus malaria.

Cai et al. demonstrated the detection of malaria using PAFC occurs at lower rates (one parasite per 0.16 mL) than traditional malaria detection systems [56]. Due to this improved sensitivity, the detection time frame can be reduced from 4 days post-inoculation to 1–2 days post inoculation [56]. In addition to showing a lower threshold for detection, Menyaev et al. demonstrated a similar low-detection limit could be achieved in an in-vivo system, providing a non-invasive alternative to current diagnostic solutions [59].

Although PAI shows promise, its use may be limited due to the use of hemozoin as a surrogate marker. Hemozoin is only produced when the parasite has matured from the sporozoite stage into the merozoite. Patients are infected with malaria in their sporophyte stage and only develop into merozoites once in the liver. Ultimately there is an unavoidable detection lag between onset of infection and presence of hemozoin. Even so, PAI provides a promising methodology for high-quality, non-invasive, and automatable processes for malaria diagnosis and monitoring. Future studies are needed to demonstrate PAI's effect on earlier detection and treatment outcomes in patients with malaria.

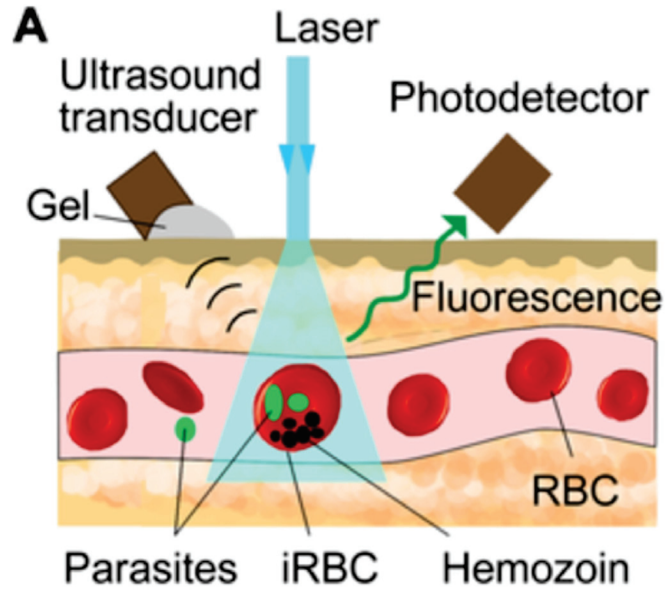

Fig. 4. Overview of photoacoustic imaging in application of malarial detection. System utilizes photoacoustic flow cytometry as demonstrated in a study performed by Cai et al. [56].

2.2.2. Bacteremia

More than 2.8 million bacterial infections occur annually in the US, costing the healthcare system more than 4.6 billion dollars per year [62]. One of the most deadly and costly complications of an infection is bacteremia. Bacteremia occurs when bacteria leaks into the blood which can lead to prolonged infection of the heart (endocarditis), sepsis, or seeding of distant organs [63]. As a result of its vast impact, bacteremia carries a 30-day mortality rate of 22% [64]. Early and accurate identification of the bacterial species is crucial to reducing antibiotic resistance, length of hospital stay, and morbidity/mortality [65]. Technology for both the identification and monitoring of pathophysiology of bacteria is critical for improving outcomes. The current gold standard for bacteremia identification relies on blood cultures [66]. Although culturing provides useful information for treatment, incubation can take tens of hours to days to develop [67]. This time-delay leads clinicians to choose broad spectrum antibiotics, which contributes to antibiotic resistance [68]. Advancements in technologies such as PCR and serology have enabled earlier detection, but faster methods are still needed.

While there are various methods of bacterial detection, current sensitivities for these technique are around 3.2×10^8 CFU/mL (colony forming units/mL) [69]. Photoacoustic imaging shows promise in providing more efficient diagnosis of bacteria in the blood. Using PA-active labels two studies were able to detect bacteria at a lower rate than current methods. Edgar et al. used dye-marked bacteriophages mixed in a bacterial solution containing Salmonella or E. Coli, which was then run through their ex-vivo PAFC system seen in Fig. 5. A sample was introduced into the system and separated into finite segmentate using mineral oil to separate the segments. Each of the segments was passed by a photoacoustic detection system. Their team was able to detect bacteria at rates as low as 1×10^5 CFU/mL [70]. Conversely, Galanzha et al. utilized golden nanorods (GNRs) to label S. Aureus, which were subsequently injected into rat models. Their in-vivo PAI system demonstrated a sensitivity as low as 0.5 CFU/mL which is substantially lower than current methods [71]. These studies provide proof of concept of in-vivo detection of bacteria, however further studies are needed to determine application to a broader range of bacteria. Ultimately, PAI could be

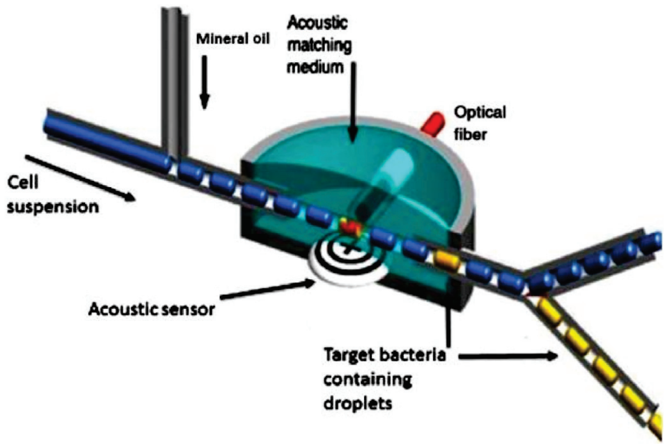

Fig. 5. Example ex-vivo photoacoustic flow cytometry setup used by Viator et al. [70].

performed at patient presentation, reducing the time for bacterial species identification significantly improving antibiotic selection, and mortality reduction.

Although PA provides promise in reduction of bacterial detection time, the aforementioned studies utilized PA-active labels, which may have some limitations in in-vivo applications. While bacteriophages, like those used in the Edgar et al. study, are more stable and more cost effective than traditional antibody markers, they are bacteria specific [70]. Thus, in clinical applications where the bacteria to be identified is unknown, the bacteriophages cannot bind rendering the dye ineffective. Zlitini et al. attempted to overcome this issue by using the non-specific bacterial metabolite maltotriose. The maltotriose is labeled with a PA-active dye and is selectively and rapidly taken up by bacteria [72]. Their study successfully demonstrated the effectiveness of their maltotriose-dye in the detection of bacterially contaminated catheters.

Similar to the Galanzha et al. study, many have proposed the use of nanoparticles. These small PA-active contrast agents are of particular interest, as they have not only shown efficacy in bacterial identification, but may also be used in bacterial eradication [73]. Kim et al. used silver-covered nanoparticles, which adhered to the bacterial surface. The PA effect then resulted in release of silver from the nanoparticles, exerting their bactericidal effect and ultimately eradicating the covered bacteria [74]. While dyes are easily implemented in ex-vivo methods, hurdles exist for the transition to in-vivo applications. Further studies are needed for evaluation of toxicity and side-effect profiles that may render the technology impractical for clinical use.

Besides bacteria-labeled methods, Thompson et al. proposed a label-free alternative. Their study demonstrated bacterial speciation via analyzing bacterial spectral responses [75]. Further expansion of this technology may provide a non-invasive, label-free application of PAI for bacteremia detection and speciation.

In a pre-clinical setting, PAI has implications in studying microbial dynamics. Cai et al. used a choryll-peptide based agent to monitor macrophage chemotaxis and bacterial uptake [76]. Fig. 6 demonstrates the phototactically labeled peptide, which is engulfed by the macrophage. When the macrophage in turn engulfs bacteria, this produces a detectible PA signal, which can be used to study and understand timing of bacterial uptake with macrophages. Additionally, Galanzha et al. demonstrated bacterial movement within the microvasculature, demonstrating endothelial attachment and extravasation within the body [71]. Such studies provide indications that PAI could be utilized to get a better understanding of bacterial mechanisms which has implications to future treatment regimens.

PAI has imaging demonstrated abilities of rapid diagnosis, provide non-invasive detection, and the potential for therapeutic applications to bacterial infections superior to current methods. Future studies are

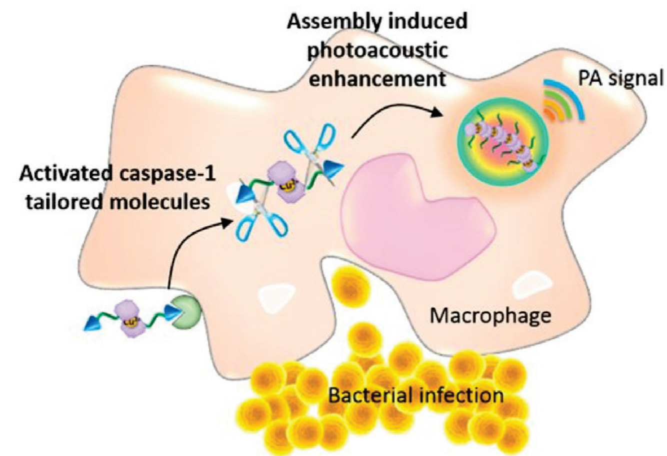

Fig. 6. Macrophage undergoing bacterial uptake inducing the production of a PA signal. Produced by Cai et al. [76].

needed to assess PA-active label safety profiles and demonstrate the quantifiable reduction in harm associated with earlier detection using PAI.

2.3. Circulating tumor cells (CTCs)

Cancer is the second leading cause of death in the United States [77]. Of cancer related deaths, 90% are attributed to metastasis [78]. This occurs when original tumor cells disseminate to distant sites within the body. These cells are known as circulating tumor cells (CTCs). Studies have shown that CTCs present in the blood result in higher rates of metastasis and thus poorer patient prognosis [79]. Consequently, detection of CTCs could provide improvement in cancer treatment and outcomes. Furthermore, trending CTC levels provide tumor recurrence monitoring and treatment responsiveness. Ultimately, preventing metastasis by CTC-targeted treatment could reduce the need for systemic treatment altogether and improve patient outcomes.

Previous studies have achieved CTC detection through a variety of methods, but various limitations have prevented their widespread use. Due to lack of reliable cellular markers and low concentration in whole blood (~0.0002–0.00075%), detection of CTCs has proved difficult [80]. Common detection methods include using cell surface markers, filtration and direct optical imaging systems (i.e. flow cytometry, raman scattering). Generally, ex-vivo methods suffer from low sample size which leads to a higher rate of false negatives [81,82]. Methods relying on cell surface markers also suffer from a high rate of false negatives due to CTC's ability to shield said markers [81,82]. In vivo optical imaging systems such as wide field fluorescence imaging and photodiagnostic infrared spectroscopy showed promise to these limitations, but due to scattering effects, these systems are restricted to superficial depths, limiting its applicability [81,82].

PAI may provide an alternative to detection of CTCs, while improving upon the aforementioned limitations. O'Brien et al. demonstrated PAI's ability to detect and separate CTCs using PAI with a two-phase microfluidic system [80]. Using an in-vitro system with melanoma CTCs in bovine blood, their system could detect the CTCs 100% of the time at a concentration of 1 CTC/μL. Importantly, they demonstrated PAI's ability to image multicellular cross sections, unlike traditional flow cytometry systems which rely on cells in a single file for analysis. Multicellular cross section analysis resembles physiologic systems implying in-vivo imaging feasibility. Fig. 7 depicts an in-vivo version of CTC detection using the multicellular cross section technique for detection. The figure shows CTC release into the blood stream due to manipulation of a tumor followed by in-vivo PA detection in the blood stream.

Multiple studies have demonstrated photoacoustic imaging of breast,

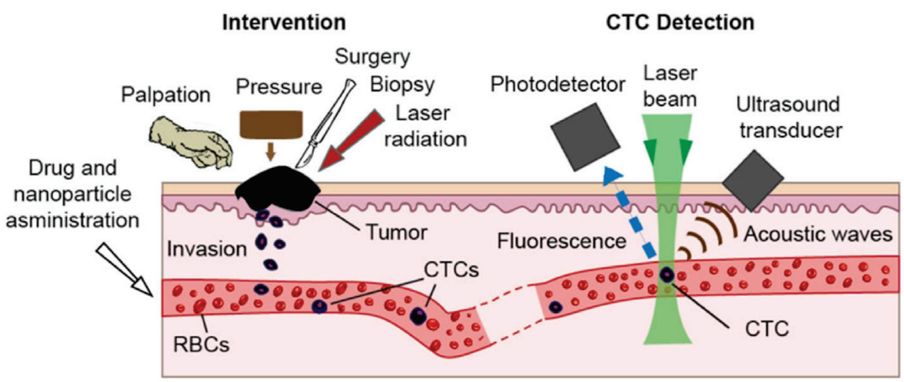

Fig. 7. In-vivo PAFC schematic for CTC detection, produced by Galanzha and Zharov [89].

prostate, ovarian and skin cancer CTCs. Certain cell lineages require labeling with PA-active dyes, yet others, such as melanoma cells contain melanin making in vivo imaging readily available. CTC tagging is generally performed through the use of metallic nanoparticles similar to those used for bacterial detection [83–86]. Other types such as magnetic nanoparticles have been used, not only producing a PA signal, but have sequestration abilities which may have treatment implications [87]. Although possibilities are broad, PAI's use may be limited due to invasive methods required for target labeling and possible side effects of such labels. Still, with the wide range of potential markers, photoacoustic imaging may be a powerful tool in CTC detection.

Despite these limitations, due to its acoustic detection, PAI's imaging depth has a large advantage over other current CTC imaging methods. Due to the improved depth, PAI enables better in-vivo utilization through visualization of deeper and larger vessels. As such, these larger vessels with higher blood flow rate allow for an increased detection throughout. In typical blood analysis, a small blood sample is extracted from the patient to be tested. Here, PAI can monitor the circulating blood for an extended period, effectively increasing the sample volume [88]. Galanzha et al. demonstrated this power by monitoring the entire blood volume of a mouse under 1 min [89]. Others observed CTCs using PAI of blood vessels at 3–4 mm depth range in human studies as proof of concept [90]. Furthermore, PAI may be applied in real-time CTC detection for procedural purposes. Jurantli et al. studied at the effect of pressure secondary to resection or incision from a tumor [88,91]. These studies demonstrate PAI ability to image deeper, larger vessels which ultimately produces a more sensitive detection of CTCs.

Finally, while PAI has great diagnostic implications, its prospect for treatment implications sets it far beyond current methods. He et al. used a 8.8 mJ/cm2 laser fluence that allowed instantaneous rupture of melanoma CTCs once they were detected, but did not damage healthy cells [91]. Galanzha et al. used CTC-targeting nanoparticles that resulted in heating-induced nanobubbles and rupturing of the CTCs [89]. In addition to mechanical destruction, the lysing of the CTCs may reveal malignant markers such as cancer antigens, thereby increasing immune detection and further destruction of the cancerous cells [91]. While limitations exist and further research needs to be performed, PAI may have an impact on improving cancer outcomes through the early detection and possibly treatment of CTCs.

3. Applications to molecular components in blood analysis

The previous section described analysis of cellular components within the blood using PAI. Here, we highlight a few examples of PAI's application for analysis of the acellular or plasma component of blood. Molecules within plasma are known as analytes, ranging in size from large proteins (e.g albumin, 15 nm) to electrolytes (eg. potassium, 0.266 nm) [92,93].Quantification of these molecules provides an abundance of information about the physiological and pathological statuses within the body. Blood analysis has been and continues to be the cornerstone of modern medicine. Currently, blood analysis requires a wide range of technologies, making testing for these molecules complex, time consuming, and expensive. PAI's application in blood analyte testing may improve the efficiency and lower the cost.

3.1. Non-invasive blood glucose monitoring

More than 34 million people in the US live with diabetes [94]. Complications from elevated blood glucose levels cost an estimated $320 million dollars to the US healthcare system annually and are rising [95]. Reliable and fast measurement of blood glucose levels is key to preventing devastating outcomes. Detection methods have progressed significantly over the years, but an accurate and non-invasive method has yet to be established.

Current detection methods often utilize disposable needles and microfluidics. While small, these invasive methods deter users from adherence to glucose monitoring [96]. A semi-implantable alternative that provides annual rather than daily needle exchange, but complexity of use and cost continue to be a barrier to use [97].

Early methods of non-invasive detection included urine glucose testing; however, reading levels were inaccurate due to the patient's large variation in hydration level. More advanced methods such as impedance spectroscopy and sonophoresis were developed, but skin irritation, among other issues, prevented their full implementation [98].An accurate and non-invasive glucose monitoring system is yet to be created.

In 2015, Pai et al. showed that photoacoustic spectroscopy (PAS) could be utilized to determine glucose levels of varying degrees [99]. Fig. 8 shows the Clark error grid (CEG) plot of glucose levels relative to the predicted concentration using photoacoustic spectroscopy (PAS) by Pai et al. Their results demonstrated PAS as a safe and effective method to measure glucose levels. Using the CEG criteria (areas A and B are clinically acceptable variation) 100% of their measurements fell within an acceptable range. Furthermore, Taknaka et al. reported a similar response and variation using differential continuous-wave photoacoustic spectroscopy and its correlation with glucose over 3 h [100].

However, not surprisingly, the more physiologically relevant tests proved difficult. Studies demonstrated a significant overlap in signal generation between glucose and other physiological substances such as water resulting in larger error in glucose concentration results. Fig. 9 demonstrates the results from Sigrist et al. who tested the in-vivo correlation of PAS for glucose levels. Their results demonstrated a larger scattering of data resulting in an R^2 value of 0.8 secondary to background signal. As such, further studies are needed to investigate these variances and solutions to improve the PA-based glucose monitoring system.

One technical obstacle in PA glucose measurement is the lack of ability to take repeatable and accurate measurements, due to the variances in skin content. Sim et al. reported concerns with signal variation due to eccrine glands. These glands produce PA-active substances with a

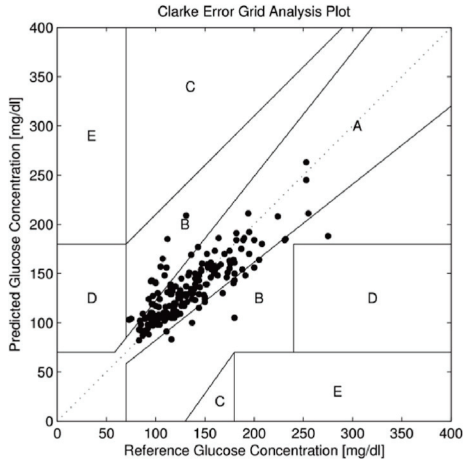

Fig. 8. Photoacoustic spectroscopy evaluation of glucose levels in solution produced in a Clark error grid. Produced by Pai et al. [99].

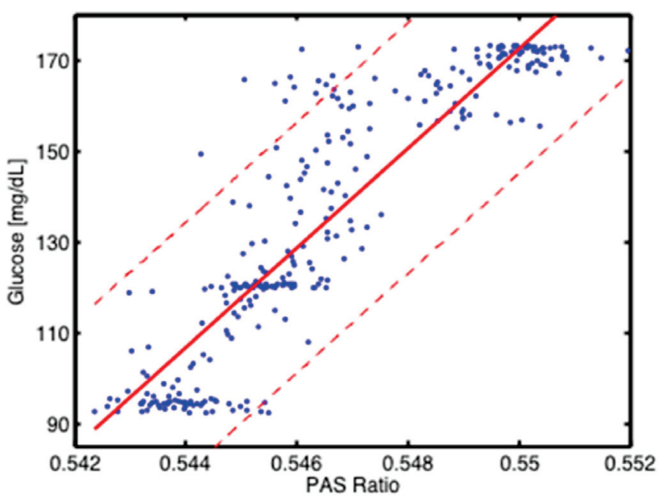

Fig. 9. Photoacoustic spectroscopy evaluation of glucose levels within the blood vs blood level extracted values. Produced by Kotmann et al. [101].

similar spectrum as glucose [98]. Their study showed that because of these glands, there was a significant variation in optical absorption across the skin, affecting the glucose measurements. Yet, their team was able to identify skin areas with high and low optical absorption, and thus use areas between the eccrine glands to produce a more accurate measurement of blood glucose content. Furthermore, these studies review physiological glucose levels. In instances of pathological conditions such a diabetes where regular exogenous insulin is in use, these glucose variations may affect PAS concentrations. While PAI needs further tuning to optimize and overcome current and future obstacles, implementation of this technology may provide a revolutionary method to non-invasive glucose testing.

3.2. Alternative analytes

While there are a vast number of analytes that can be potentially measured by PAI, this paper discusses only a few pilot studies in PAI analyte testing. To demonstrate the range of PA's applicability, we've selected analyte testing in the following categories: blood proteins, pharmaceuticals, and electrolytes. As previously mentioned, current analyte detection and measurement generally requires an individual test for each analyte of interest. Therefore, using a photoacoustic system for the testing of all analytes may provide a standardized method allowing for simplified and cost-effective blood analysis.

A few studies have shown efficacy in detection of blood protein concentrations. For example, carbon monoxide, an odorless, colorless gas causes a toxic conformational change to hemoglobin, forming the blood protein carboxyhemoglobin. Due to its rarity and subtle clinical characteristics, diagnosis can be difficult [102]. Chen and Peters et al. demonstrated PAI's ability to detect carboxyhemoglobin's blood level and characterize its kinetics [103,104]. Similarly, methemoglobin (metHb) is a toxic blood protein formed from the use of medications in the nitrite class. Like carboxyhemoglobin, testing for metHb can be arduous. Furthermore, diagnosis and treatment are time-sensitive. Multiple studies have shown PAI to be a viable option for expedited and in-vivo testing for metHb [105,106]. A third example of protein detection with PAI is bilirubin. Hyperbilirubinemia is a common finding in newborns. In most, it resolves naturally, but in certain instances it requires medical intervention. Thus, routine care involves regular bilirubin level checks. Due to the sensitivity of the pediatric population, noninvasive transcutaneous analysis is the preferred detection method. Current methods utilize optical imaging systems, which have proven effective for screening tools, but have depth limitations as mentioned previously [107]. Zhou et al. illustrated PAI's effectiveness in the detection of bilirubin in a bovine blood phantom solution [108]. Fig. 10 demonstrates their results by showing a significant correlation between concentration of bilirubin and calculated concentration based on photoacoustic signal intensity. These studies show PAI's potential to observe and quantify proteins within the blood which may have implications for biomarker detection and monitoring.

Smaller molecules, such as pharmaceuticals, could also be monitored by PAI. Jeevarathinam et al. detected the drug heparin using a PAI system [109–111]. Similarly, Yim et al. utilized polydopamine nanocapsules (PNCs) with molecular dyes to enhance PA-mediated heparin detection [112]. Their studies also provided drug effectiveness data, by comparing rheology parameters extracted from the PA data with conventional activated coagulation time (ACT) measurements. They proposed PAI may play a role in areas such as invasive-intraoperative continuous clotting measures for cardiac surgeries. Fig. 11 shows measured and simulated photoacoustic intensities of heparin and their resulting ACTs as a function of heparin concentration.

In another study, Furdella et al. used PAI to detect and measure the drug Dil (1,1′-dioctadecyl-3,3,3′,3′- tetramethylindocarbocyanine perchlorate), a surrogate for rapamycin in DES (drug eluting stents) [114]. Their team monitored porcine coronary arteries after drug injection of the drug and found a concentration-dependent PA signal. These data may be used to confirm that the DES is providing a drug concentration within the desired therapeutic range. Lastly, Taruttis et al. performed pharmacokinetic studies using PAI with indocyanine green (ICG) dye [115]. They performed in-vivo PAI of the ischiatic vein of a mouse and characterized the circulation kinetics of ICG. These studies show PAI's ability to identify and quantify pharmaceuticals, which may ultimately be used in pharmacokinetic studies.

Finally, there have been a few studies demonstrating ion concentration detection. Cash et al. used optode nanosensors in a photoacoustic

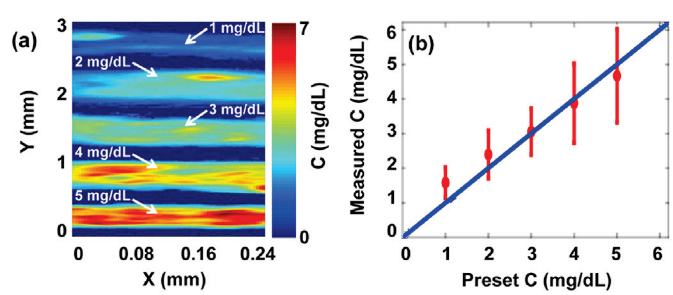

Fig. 10. Photoacoustic imaging and quantification of bilirubin samples of varying concentration in phantoms. Produced by Zhou et al. [108].

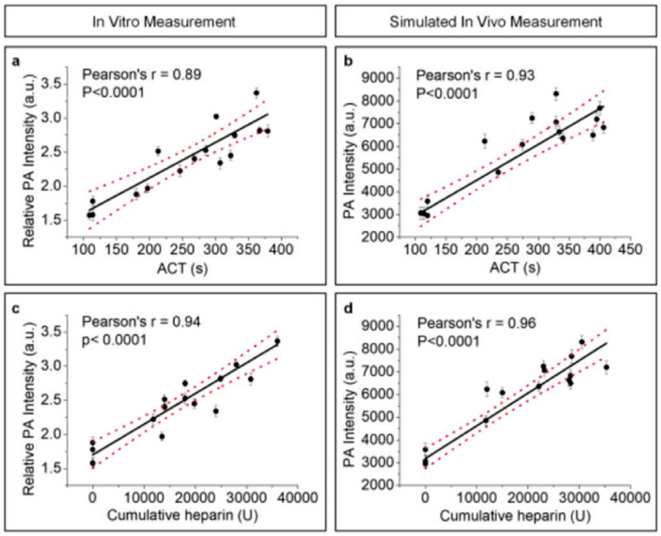

Fig. 11. Photoacoustic analysis of heparin using an in vitro (human blood) PAI system. The above graphs demonstrate a statistically significant correlation between PA measurements and ACT clotting measurements and heparin units. Produced by Zhou et al. [113].

system for detection of lithium [116]. Using complex formulated optode nanosensors, they showed a concentration-dependent photoacoustic signal using a chicken skin phantom. Lee et al. used a similar method with an ion-selective optode to perform an ex-vivo analysis of potassium concentration in a phantom [117]. While neither of these studies demonstrated in-vivo effectiveness, their studies provide a proof-of-concept for ion detection using PAI, lending to potential electrolyte concentration analysis in the future.

These studies demonstrated the wide range of existing applications for PAI in blood analysis and showed the potential for many new applications. Limitations from background signals, penetration depth, signal consistency and measurement accuracy require further work, but do not prevent the fast development and clinical implementation of this exciting technology in blood analysis.

4. Conclusion

As a ubiquitous fluid within the body, blood has broad implications in detection, monitoring and treatment of many pathophysiological processes. Due to PAI's superior depth of penetration and non-invasive nature, it has a wide range of applications in blood analysis. Its versatility in detecting many targets with a single system provides advantage over the current olio of systems required to test for individual targets. Furthermore, PAI's non-invasive nature lends to more accurate examination of pathophysiologic status within an undisturbed biological subject. The combination of these features makes PAI prime for enhanced utilization in preclinical settings and translation into more clinical settings.

Although improved over pure optical imaging systems, limitations still exist for PAI's application to blood analysis. Background noises from intrinsic chromophores such as eccrine gland production and hemoglobin provide difficulty in identifying target signals in in-vivo settings, yet varying studies are under way to develop solutions [118]. Additionally, pure label-free detection of many blood analytes may prove difficult. The use of PA-active labels will require rigorous toxicologic testing, but ultimately may provide advantages in more sophisticated imaging of targets in in-vivo settings. Besides, some studies continue to investigate photoacoustic spectroscopy for label-free analysis for a broader range of analytes [119]. While challenges exist, studies have enlightened possible solutions that continue to show a positive future for PAI's application to blood analysis.

While challenges exist, there are a significant number of studies demonstrating the impressive impact PAI could have on blood analysis. Its label free signal from hemoglobin lends itself well to further implementation in in-vivo monitoring of sickle cell disease. Its in-vivo monitoring of blood flow has implications for point of care detection in infectious diseases and its tunable wavelength and wide range of PA-active labels may enable for detection of a vast number of analytes.

Overall, photoacoustic imaging provides great promise in the application to blood analysis. As blood analysis is a cornerstone for modern medicine this technology could have significant impacts in the way blood is studied in pre-clinical labs and how blood is analyzed and monitored in the clinical setting. We expect a progression of PAI integration in blood analysis using photoacoustic imaging in future years as the technology evolves.

Patient consent

No humans subjects were used in the production of this manuscript.

Ethical approval and informed consent

No human or animal subjects were used in the production of this manuscript.

Funding source

This research was funded by The United States National Institutes of Health (NIH) grants R38HL143612, R21EB027981, R21 EB027304, RF1 NS115581 (BRAIN Initiative), R01 NS111039, R01 EB028143; The United States National Science Foundation (NSF) CAREER award 2144788; and Chan Zuckerberg Initiative Grant (2020-226178).

Author contribution to study

Mitchell Veverka: conceptualization, literature review, writing, reviewing, and editing. Luca Menozzi: contribution to literature review and input on further conceptualization, reviewing and editing.

Copyrights

Declaration of competing interest

The authors declare that they have no known competing financial interests or personal relationships that could have appeared to influence the work reported in this paper.

References

[1] Nadler SB, Hidalgo SJ, Bloch T. Prediction of blood volume in normal human adults. Surgery 1962;51:224–32.

[2] Underwood J, Marks M, Collins S, Logan S, Pollara G. Intravenous catheter-related adverse events exceed drug-related adverse events in outpatient parenteral antimicrobial therapy. J Antimicrob Chemother 2019;74:787–90. https://doi.org/10.1093/jac/dky474.

[3] Parasuraman S, Raveendran R, Kesavan R. Blood sample collection in small laboratory animals. J Pharmacol Pharmacother 2010;1:87–93. https://doi.org/10.4103/0976-500X.72350.

[4] Groothuis FA, Heringa MB, Nicol B, Hermens JLM, Blaauboer BJ, Kramer NI. Dose metric considerations in in vitro assays to improve quantitative in vitro-in vivo dose extrapolations. Toxicology 2015;332:30–40. https://doi.org/10.1016/j.tox.2013.08.012.
[5] Hooiveld M, Roosendaal G, Vianen M, van den Berg M, Bijlsma J, Lafeber F. Blood-induced joint damage: longterm effects in vitro and in vivo. J Rheumatol 2003;30:339–44.
[6] Dehouck MP, Jolliet-Riant P, Brée F, Fruchart JC, Cecchelli R, Tillement JP. Drug transfer across the blood-brain barrier: correlation between in vitro and in vivo models. J Neurochem 1992;58:1790–7. https://doi.org/10.1111/j.1471-4159.1992.tb10055.x.
[7] Centers for Medicare & Medicaid Services, CMS Clinical Labratory Amendments. CMS clinical labratory amendments statistical tables and graphs. n.d. https://www.cms.gov/Regulations-and-Guidance/Legislation/CLIA/CLIA_Statistical_Tables_Graphs. [Accessed 26 October 2021]. accessed
[8] Hong B, Zu Y. Detecting circulating tumor cells: current challenges and new trends. Theranostics 2013;3:377–94. https://doi.org/10.7150/thno.5195.
[9] Mahram M, Oveisi S, Jaberi N. Trans-cutaneous bilirubinometery versus serum bilirubin in neonatal jaundice. Acta Med Iran 2015;53:764–9.
[10] Jubran A. Pulse oximetry. Crit Care 2015;19:272. https://doi.org/10.1186/s13054-015-0984-8.
[11] Kraitl J, Klinger D, Fricke D, Timm U, Ewald H. Non-invasive measurement of blood components. In: Mukhopadhyay SC, Jayasundera KP, Fuchs A, editors. Advancement in sensing technology, vol. 1. Berlin, Heidelberg: Springer Berlin Heidelberg; 2013. p. 237–62. https://doi.org/10.1007/978-3-642-32180-1_14.
[12] Lyamshev LM. Optoacoustic sources of sound. Sov Phys Usp 1981;24:977–95. https://doi.org/10.1070/PU1981v024n12ABEH004757.
[13] Borg RE, Rochford J. Molecular photoacoustic contrast agents: design principles & applications. Photochem Photobiol 2018;94:1175–209. https://doi.org/10.1111/php.12967.
[14] Weber J, Beard PC, Bohndiek SE. Contrast agents for molecular photoacoustic imaging. Nat Methods 2016;13:639–50. https://doi.org/10.1038/nmeth.3929.
[15] Luke GP, Nam SY, Emelianov SY. Optical wavelength selection for improved spectroscopic photoacoustic imaging. Photoacoustics 2013;1:36–42. https://doi.org/10.1016/j.pacs.2013.08.001.
[16] Xia J, Yao J, Wang LV. Photoacoustic tomography: principles and advances. Electromagn Waves 2014;147:1–22. https://doi.org/10.2528/pier14032303.
[17] Sharma A, Srishti Periyasamy V, Pramanik M. Photoacoustic imaging depth comparison at 532-, 800-, and 1064-nm wavelengths: Monte Carlo simulation and experimental validation. J Biomed Opt 2019;24:1. https://doi.org/10.1117/1.JBO.24.12.121904.
[18] Fouquet C, Gilles J-F, Heck N, Dos Santos M, Schwartzmann R, Cannaya V, et al. Improving axial resolution in confocal microscopy with new high refractive index mounting media. PLoS One 2015;10:e0121096. https://doi.org/10.1371/journal.pone.0121096.
[19] Reihani SNS, Oddershede LB. Confocal microscopy of thick specimens. J Biomed Opt 2009;14:030513. https://doi.org/10.1117/1.3156813.
[20] Spaide RF, Otto T, Caujolle S, Kübler J, Aumann S, Fischer J, et al. Lateral resolution of a commercial optical coherence tomography instrument. Transl Vis Sci Technol 2022;11:28. https://doi.org/10.1167/tvst.11.1.28.
[21] Sharma U, Chang EW, Yun SH. Long-wavelength optical coherence tomography at 1.7 microm for enhanced imaging depth. Opt Express 2008;16:19712–23. https://doi.org/10.1364/oe.16.019712.
[22] Opilik L, Schmid T, Zenobi R. Modern Raman imaging: vibrational spectroscopy on the micrometer and nanometer scales. Annu Rev Anal Chem 2013;6:379–98. https://doi.org/10.1146/annurev-anchem-062012-092646.
[23] Hill AH, Manifold B, Fu D. Tissue imaging depth limit of stimulated Raman scattering microscopy. Biomed Opt Express 2020;11:762–74. https://doi.org/10.1364/BOE.382396.
[24] Hu S, Wang LV. Optical-resolution photoacoustic microscopy: auscultation of biological systems at the cellular level. Biophys J 2013;105:841–7. https://doi.org/10.1016/j.bpj.2013.07.017.
[25] Park S, Lee C, Kim J, Kim C. Acoustic resolution photoacoustic microscopy. Biomed Eng Lett 2014;4:213–22. https://doi.org/10.1007/s13534-014-0153-z.
[26] Zhou Y, Yao J, Wang LV. Tutorial on photoacoustic tomography. J Biomed Opt 2016;21:61007. https://doi.org/10.1117/1.JBO.21.6.061007.
[27] Periyasamy V, Das N, Sharma A, Pramanik M. 1064 nm acoustic resolution photoacoustic microscopy. J Biophot 2019;12:e201800357. https://doi.org/10.1002/jbio.201800357.
[28] Tian C, Zhang C, Zhang H, Xie D, Jin Y. Spatial resolution in photoacoustic computed tomography. Rep Prog Phys 2021;84. https://doi.org/10.1088/1361-6633/abdab9.
[29] Moothanchery M, Bi R, Kim JY, Jeon S, Kim C, Olivo M. Optical resolution photoacoustic microscopy based on multimode fibers. Biomed Opt Express 2018;9:1190–7. https://doi.org/10.1364/BOE.9.001190.
[30] Liu W, Yao J. Photoacoustic microscopy: principles and biomedical applications. Biomed Eng Lett 2018;8:203–13. https://doi.org/10.1007/s13534-018-0067-2.
[31] Wang LV, Yao J. A practical guide to photoacoustic tomography in the life sciences. Nat Methods 2016;13:627–38. https://doi.org/10.1038/nmeth.3925.
[32] Moothanchery M, Dev K, Balasundaram G, Bi R, Olivo M. Acoustic resolution photoacoustic microscopy based on microelectromechanical systems scanner. J Biophot 2020;13:e201960127. https://doi.org/10.1002/jbio.201960127.
[33] Prakash J, Sanny D, Kalva SK, Pramanik M, Yalavarthy PK. Fractional regularization to improve photoacoustic tomographic image reconstruction. IEEE Trans Med Imag 2019;38:1935–47. https://doi.org/10.1109/TMI.2018.2889314.
[34] Rao B, Zhang R, Li L, Shao J-Y, Wang LV. Photoacoustic imaging of voltage responses beyond the optical diffusion limit. Sci Rep 2017;7:2560. https://doi.org/10.1038/s41598-017-02458-w.
[35] Li R, Wang P, Lan L, Lloyd FP, Goergen CJ, Chen S, et al. Assessing breast tumor margin by multispectral photoacoustic tomography. Biomed Opt Express 2015;6:1273–81. https://doi.org/10.1364/BOE.6.001273.
[36] Wang LV, Gao L. Photoacoustic microscopy and computed tomography: from bench to bedside. Annu Rev Biomed Eng 2014;16:155–85. https://doi.org/10.1146/annurev-bioeng-071813-104553.
[37] Hu S, Maslov K, Wang LV. Noninvasive label-free imaging of microhemodynamics by optical-resolution photoacoustic microscopy. Opt Express 2009;17:7688–93. https://doi.org/10.1364/oe.17.007688.
[38] Matsumoto Y, Asao Y, Yoshikawa A, Sekiguchi H, Takada M, Furu M, et al. Label-free photoacoustic imaging of human palmar vessels: a structural morphological analysis. Sci Rep 2018;8:786. https://doi.org/10.1038/s41598-018-19161-z.
[39] Mamalis A, Ho D, Jagdeo J. Optical coherence tomography imaging of normal, chronologically aged, photoaged and photodamaged skin: a systematic review. Dermatol Surg 2015;41:993–1005. https://doi.org/10.1097/DSS.0000000000000457.
[40] Vu T, Razansky D, Yao J. Listening to tissues with new light: recent technological advances in photoacoustic imaging. J Opt 2019;21. https://doi.org/10.1088/2040-8986/ab3b1a.
[41] Gurcan MN, Boucheron LE, Can A, Madabhushi A, Rajpoot NM, Yener B. Histopathological image analysis: a review. IEEE Rev Biomed Eng 2009;2:147–71. https://doi.org/10.1109/RBME.2009.2034865.
[42] Wittekind D. Traditional staining for routine diagnostic pathology including the role of tannic acid. 1. Value and limitations of the hematoxylin-eosin stain. Biotech Histochem 2003;78:261–70. https://doi.org/10.1080/10520290310001633725.
[43] Milner PF. Oxygen transport in sickle cell anemia. Arch Intern Med 1974;133:565–72. https://doi.org/10.1001/archinte.1974.00320160059006.
[44] Manwani D, Frenette PS. Vaso-occlusion in sickle cell disease: pathophysiology and novel targeted therapies. Blood 2013;122:3892–8. https://doi.org/10.1182/blood-2013-05-498311.
[45] Ballas SK, Smith ED. Red blood cell changes during the evolution of the sickle cell painful crisis. Blood 1992;79:2154–63.
[46] Jacob E, American Pain Society. Pain management in sickle cell disease. Pain Manag Nurs 2001;2:121–31. https://doi.org/10.1053/jpmn.2001.26297.
[47] Strohm EM, Berndl ESL, Kolios MC. Probing red blood cell morphology using high-frequency photoacoustics. Biophys J 2013;105:59–67. https://doi.org/10.1016/j.bpj.2013.05.037.
[48] Biswas D, Gorey A, Chen GCK, Sharma N, Vasudevan S. Investigation of diseases through red blood cells' shape using photoacoustic response technique. In: Tuchin VV, Larin KV, Leahy MJ, Wang RK, editors. Dynamics and fluctuations in biomedical photonics XII, 9322. SPIE; 2015. 93220K. https://doi.org/10.1117/12.2079185.
[49] Cai C, Nedosekin DA, Menyaev YA, Sarimollaoglu M, Proskurnin MA, Zharov VP. Photoacoustic flow cytometry for single sickle cell detection in vitro and in vivo. Anal Cell Pathol 2016;2016:2642361. https://doi.org/10.1155/2016/2642361.
[50] Galanzha EI, Zharov VP. In vivo photoacoustic and photothermal cytometry for monitoring multiple blood rheology parameters. Cytometry 2011;79:746–57. https://doi.org/10.1002/cyto.a.21133.
[51] GBD results tool | GHDx. n.d. http://ghdx.healthdata.org/gbd-results-tool. [Accessed 1 December 2021]. accessed
[52] Disease burden from communicable, maternal, neonatal and nutritional diseases - our World in Data. n.d. https://ourworldindata.org/grapher/disease-burden-from-communicable-diseases?country=%7EOWID_WRL. [Accessed 1 December 2021]. accessed
[53] The top 10 causes of death. n.d. https://www.who.int/news-room/fact-sheets/detail/the-top-10-causes-of-death. [Accessed 1 December 2021]. accessed
[54] Malaria. n.d. https://www.who.int/news-room/fact-sheets/detail/malaria. [Accessed 19 September 2021]. accessed
[55] Global malaria programme. n.d. https://www.who.int/teams/global-malaria-programme. [Accessed 12 July 2022]. accessed
[56] Cai C, Carey KA, Nedosekin DA, Menyaev YA, Sarimollaoglu M, Galanzha EI, et al. In vivo photoacoustic flow cytometry for early malaria diagnosis. Cytometry 2016;89:531–42. https://doi.org/10.1002/cyto.a.22854.
[57] CDC - malaria - about malaria - biology. n.d. https://www.cdc.gov/malaria/about/biology/index.html#. [Accessed 12 July 2022]. accessed
[58] Egan TJ. Recent advances in understanding the mechanism of hemozoin (malaria pigment) formation. J Inorg Biochem 2008;102:1288–99. https://doi.org/10.1016/j.jinorgbio.2007.12.004.
[59] Menyaev YA, Carey KA, Nedosekin DA, Sarimollaoglu M, Galanzha EI, Stumhofer JS, et al. Preclinical photoacoustic models: application for ultrasensitive single cell malaria diagnosis in large vein and artery. Biomed Opt Express 2016;7:3643–58. https://doi.org/10.1364/BOE.7.003643.
[60] Trampuz A, Jereb M, Muzlovic I, Prabhu RM. Clinical review: severe malaria. Crit Care 2003;7:315–23. https://doi.org/10.1186/cc2183.
[61] Stauffer WM, Cartwright CP, Olson DA, Juni BA, Taylor CM, Bowers SH, et al. Diagnostic performance of rapid diagnostic tests versus blood smears for malaria in US clinical practice. Clin Infect Dis 2009;49:908–13. https://doi.org/10.1086/605436.
[62] Nelson RE, Hatfield KM, Wolford H, Samore MH, Scott RD, Reddy SC, et al. National estimates of healthcare costs associated with multidrug-resistant

bacterial infections among hospitalized patients in the United States. Clin Infect Dis 2021;72:S17–26. https://doi.org/10.1093/cid/ciaa1581.

[63] Keynan Y, Rubinstein E. Staphylococcus aureus bacteremia, risk factors, complications, and management. Crit Care Clin 2013;29:547–62. https://doi.org/10.1016/j.ccc.2013.03.008.

[64] Nielsen SL. The incidence and prognosis of patients with bacteremia. Dan Med J 2015;62.

[65] Liu VX, Fielding-Singh V, Greene JD, Baker JM, Iwashyna TJ, Bhattacharya J, et al. The timing of early antibiotics and hospital mortality in sepsis. Am J Respir Crit Care Med 2017;196:856–63. https://doi.org/10.1164/rccm.201609-1848OC.

[66] Magadia RR, Weinstein MP. Laboratory diagnosis of bacteremia and fungemia. Infect Dis Clin 2001;15:1009–24. https://doi.org/10.1016/s0891-5520(05)70184-7.

[67] Pardo J, Klinker KP, Borgert SJ, Trikha G, Rand KH, Ramphal R. Time to positivity of blood cultures supports antibiotic de-escalation at 48 hours. Ann Pharmacother 2014;48:33–40. https://doi.org/10.1177/1060028013511229.

[68] Mayer KH. The epidemiology of antibiotic resistance in hospitals. J Antimicrob Chemother 1986;18(Suppl C). https://doi.org/10.1093/jac/18.supplement_c.223. 223–33.

[69] Wang M-C, Lin W-H, Yan J-J, Fang H-Y, Kuo T-H, Tseng C-C, et al. Early identification of microorganisms in blood culture prior to the detection of a positive signal in the BACTEC FX system using matrix-assisted laser desorption/ionization-time of flight mass spectrometry. J Microbiol Immunol Infect 2015;48:419–24. https://doi.org/10.1016/j.jmii.2013.10.006.

[70] Edgar RH, Cook J, Noel C, Minard A, Sajewski A, Fitzpatrick M, et al. Bacteriophage-mediated identification of bacteria using photoacoustic flow cytometry. J Biomed Opt 2019;24:1–7. https://doi.org/10.1117/1.JBO.24.11.115003.

[71] Galanzha EI, Shashkov E, Sarimollaoglu M, Beenken KE, Basnakian AG, Shirtliff ME, et al. In vivo magnetic enrichment, photoacoustic diagnosis, and photothermal purging of infected blood using multifunctional gold and magnetic nanoparticles. PLoS One 2012;7:e45557. https://doi.org/10.1371/journal.pone.0045557.

[72] Zlitni A, Gowrishankar G, Steinberg I, Haywood T, Sam Gambhir S. Maltotriose-based probes for fluorescence and photoacoustic imaging of bacterial infections. Nat Commun 2020;11:1250. https://doi.org/10.1038/s41467-020-14985-8.

[73] de la Zerda A, Kim J-W, Galanzha EI, Gambhir SS, Zharov VP. Advanced contrast nanoagents for photoacoustic molecular imaging, cytometry, blood test and photothermal theranostics. Contrast Media Mol Imaging 2011;6:346–69. https://doi.org/10.1002/cmmi.455.

[74] Kim T, Zhang Q, Li J, Zhang L, Jokerst JV. A gold/silver hybrid nanoparticle for treatment and photoacoustic imaging of bacterial infection. ACS Nano 2018;12:5615–25. https://doi.org/10.1021/acsnano.8b01362.

[75] Thompson SE, Foster NS, Johnson TJ, Valentine NB, Amonette JE. Identification of bacterial spores using statistical analysis of Fourier transform infrared photoacoustic spectroscopy data. Appl Spectrosc 2003;57:893–9. https://doi.org/10.1366/000370203322258832.

[76] Cai Q, Fei Y, Hu L, Huang Z, Li L-L, Wang H. Chemotaxis-instructed intracellular Staphylococcus aureus infection detection by a targeting and self-assembly signal-enhanced photoacoustic probe. Nano Lett 2018;18:6229–36. https://doi.org/10.1021/acs.nanolett.8b02286.

[77] FastStats - deaths and mortality n.d. https://www.cdc.gov/nchs/fastats/deaths.htm. [Accessed 15 December 2021]. accessed.

[78] Chaffer CL, Weinberg RA. A perspective on cancer cell metastasis. Science 2011;331:1559–64. https://doi.org/10.1126/science.1203543.

[79] Paterlini-Brechot P, Benali NL. Circulating tumor cells (CTC) detection: clinical impact and future directions. Cancer Lett 2007;253:180–204. https://doi.org/10.1016/j.canlet.2006.12.014.

[80] O'Brien CM, Rood KD, Bhattacharyya K, DeSouza T, Sengupta S, Gupta SK, et al. Capture of circulating tumor cells using photoacoustic flowmetry and two phase flow. J Biomed Opt 2012;17:061221. https://doi.org/10.1117/1.JBO.17.6.061221.

[81] Shen Z, Wu A, Chen X. Current detection technologies for circulating tumor cells. Chem Soc Rev 2017;46:2038–56. https://doi.org/10.1039/c6cs00803h.

[82] Habli Z, AlChamaa W, Saab R, Kadara H, Khraiche ML. Circulating tumor cell detection technologies and clinical utility: challenges and opportunities. Cancers 2020;12. https://doi.org/10.3390/cancers12071930.

[83] Lusk JF, Miranda C, Howell M, Chrest M, Eshima J, Smith BS. Photoacoustic flow system for the detection of ovarian circulating tumor cells utilizing copper sulfide nanoparticles. ACS Biomater Sci Eng 2019;5:1553–60. https://doi.org/10.1021/acsbiomaterials.8b01217.

[84] Sobral-Filho RG, DeVorkin L, Macpherson S, Jirasek A, Lum JJ, Brolo AG. Ex vivo detection of circulating tumor cells from whole blood by direct nanoparticle visualization. ACS Nano 2018;12:1902. https://doi.org/10.1021/acsnano.7b08813. –9.

[85] Nedosekin DA, Juratli MA, Sarimollaoglu M, Moore CL, Rusch NJ, Smeltzer MS, et al. Photoacoustic and photothermal detection of circulating tumor cells, bacteria and nanoparticles in cerebrospinal fluid in vivo and ex vivo. J Biophot 2013;6:523–33. https://doi.org/10.1002/jbio.201200242.

[86] Viator JA, Gupta S, Goldschmidt BS, Bhattacharyyal K, Kannan R, Shukla R, et al. Gold nanoparticle mediated detection of prostate cancer cells using photoacoustic flowmetry with optical reflectance. J Biomed Nanotechnol 2010;6:187–91. https://doi.org/10.1166/jbn.2010.1105.

[87] Wei C, Xia J, Pelivanov I, Jia C, Huang S-W, Hu X, et al. Magnetomotive photoacoustic imaging: in vitro studies of magnetic trapping with simultaneous photoacoustic detection of rare circulating tumor cells. J Biophot 2013;6:513–22. https://doi.org/10.1002/jbio.201200221.

[88] Juratli MA, Sarimollaoglu M, Siegel ER, Nedosekin DA, Galanzha EI, Suen JY, et al. Real-time monitoring of circulating tumor cell release during tumor manipulation using in vivo photoacoustic and fluorescent flow cytometry. Head Neck 2014;36:1207–15. https://doi.org/10.1002/hed.23439.

[89] Galanzha EI, Zharov VP. Circulating tumor cell detection and capture by photoacoustic flow cytometry in vivo and ex vivo. Cancers 2013;5:1691–738. https://doi.org/10.3390/cancers5041691.

[90] Hai P, Qu Y, Li Y, Zhu L, Shmuylovich L, Cornelius LA, et al. Label-free high-throughput photoacoustic tomography of suspected circulating melanoma tumor cells in patients in vivo. J Biomed Opt 2020;25:1–17. https://doi.org/10.1117/1.JBO.25.3.036002.

[91] He Y, Wang L, Shi J, Yao J, Li L, Zhang R, et al. In vivo label-free photoacoustic flow cytography and on-the-spot laser killing of single circulating melanoma cells. Sci Rep 2016;6:39616. https://doi.org/10.1038/srep39616.

[92] Tojo A, Kinugasa S. Mechanisms of glomerular albumin filtration and tubular reabsorption. Internet J Nephrol 2012;2012:481520. https://doi.org/10.1155/2012/481520.

[93] Huang LY, Catterall WA, Ehrenstein G. Selectivity of cations and nonelectrolytes for acetylcholine-activated channels in cultured muscle cells. J Gen Physiol 1978;71:397–410. https://doi.org/10.1085/jgp.71.4.397.

[94] National diabetes statistics report. CDC; 2020. n.d. https://www.cdc.gov/diabetes/data/statistics-report/index.html. [Accessed 19 December 2021]. accessed

[95] American Diabetes Association. Economic costs of diabetes in the U.S. in 2017. Diabetes Care 2018;41:917–28. https://doi.org/10.2337/dci18-0007.

[96] Al Hayek AA, Robert AA, Babli S, Almonea K, Al Dawish MA. Fear of self-injecting and self-testing and the related risk factors in adolescents with type 1 diabetes: a cross-sectional study. Diabetes Ther 2017;8:75–83. https://doi.org/10.1007/s13300-016-0221-8.

[97] Rodbard D. Continuous glucose monitoring: a review of successes, challenges, and opportunities. Diabetes Technol Therapeut 2016;18(Suppl 2). https://doi.org/10.1089/dia.2015.0417. S3–13.

[98] Sim JY, Ahn C-G, Jeong E-J, Kim BK. In vivo microscopic photoacoustic spectroscopy for non-invasive glucose monitoring invulnerable to skin secretion products. Sci Rep 2018;8:1059. https://doi.org/10.1038/s41598-018-19340-y.

[99] Pai PP, Sanki PK, Sarangi S, Banerjee S. Modelling, verification, and calibration of a photoacoustics based continuous non-invasive blood glucose monitoring system. Rev Sci Instrum 2015;86:064901. https://doi.org/10.1063/1.4922416.

[100] Tanaka Y, Tajima T, Seyama M, Waki K. Differential continuous wave photoacoustic spectroscopy for non-invasive glucose monitoring. IEEE Sensor J 2020;20:4453–8. https://doi.org/10.1109/JSEN.2019.2962251.

[101] Kottmann J, Rey JM, Sigrist MW. Mid-infrared photoacoustic detection of glucose in human skin: towards non-invasive diagnostics. Sensors 2016;16. https://doi.org/10.3390/s16101663.

[102] Walker E, Hay A. Carbon monoxide poisoning. BMJ 1999;319:1082–3. https://doi.org/10.1136/bmj.319.7217.1082.

[103] Chen Z, Yang S, Xing D. In vivo detection of hemoglobin oxygen saturation and carboxyhemoglobin saturation variations with photoacoustic microscopy. In: Luo Q, Gu Y, Li XD, editors. Optics in Health care and biomedical optics V, vol. 8553. SPIE; 2012. 85532U. https://doi.org/10.1117/12.999746.

[104] Peters KS, Watson T, Logan T. Photoacoustic calorimetry study of human carboxyhemoglobin. J Am Chem Soc 1992;114:4276–8. https://doi.org/10.1021/ja00037a035.

[105] Peterson RW, Kadugodinandareddy K, Karunakaran V, Whitney C, Ling J, Ye JY. Utilizing an open-microcavity optoacoustic sensor for spectroscopic determination of methemoglobin concentration. In: Tromberg BJ, Yodh AG, Sevick-Muraca EM, Alfano RR, editors. Optical tomography and spectroscopy of tissue XI, vol. 9319. SPIE; 2015. 93191N. https://doi.org/10.1117/12.2080119.

[106] Tang M, Zhou Y, Zhang R, Wang LV. Noninvasive photoacoustic microscopy of methemoglobin in vivo. J Biomed Opt 2015;20:036007. https://doi.org/10.1117/1.JBO.20.3.036007.

[107] el-Beshbishi SN, Shattuck KE, Mohammad AA, Petersen JR. Hyperbilirubinemia and transcutaneous bilirubinometry. Clin Chem 2009;55:1280–7. https://doi.org/10.1373/clinchem.2008.121889.

[108] Zhou Y, Zhang C, Yao D-K, Wang LV. Photoacoustic microscopy of bilirubin in tissue phantoms. J Biomed Opt 2012;17:126019. https://doi.org/10.1117/1.JBO.17.12.126019.

[109] Jeevarathinam AS, Pai N, Huang K, Hariri A, Wang J, Bai Y, et al. A cellulose-based photoacoustic sensor to measure heparin concentration and activity in human blood samples. Biosens Bioelectron 2019;126:831–7. https://doi.org/10.1016/j.bios.2018.11.052.

[110] Wang J, Jeevarathinam AS, Humphries K, Jhunjhunwala A, Chen F, Hariri A, et al. A mechanistic investigation of methylene blue and heparin interactions and their photoacoustic enhancement. Bioconjugate Chem 2018;29:3768–75. https://doi.org/10.1021/acs.bioconjchem.8b00639.

[111] Wang J, Chen F, Arconada-Alvarez SJ, Hartanto J, Yap L-P, Park R, et al. A nanoscale tool for photoacoustic-based measurements of clotting time and therapeutic drug monitoring of heparin. Nano Lett 2016;16:6265–71. https://doi.org/10.1021/acs.nanolett.6b02557.

[112] Yim W, Takemura K, Zhou J, Zhou J, Jin Z, Borum RM, et al. Enhanced photoacoustic detection of heparin in whole blood via melanin nanocapsules carrying molecular agents. ACS Nano 2021. https://doi.org/10.1021/acsnano.1c08178.

[113] Zhou J, Yim W, Zhou J, Jin Z, Xu M, Mantri Y, et al. A fiber optic photoacoustic sensor for real-time heparin monitoring. Biosens Bioelectron 2022;196:113692. https://doi.org/10.1016/j.bios.2021.113692.

[114] Furdella KJ, Witte RS, Vande Geest JP. Tracking delivery of a drug surrogate in the porcine heart using photoacoustic imaging and spectroscopy. J Biomed Opt 2017; 22:41016. https://doi.org/10.1117/1.JBO.22.4.041016.

[115] Taruttis A, Morscher S, Burton NC, Razansky D, Ntziachristos V. Fast multispectral optoacoustic tomography (MSOT) for dynamic imaging of pharmacokinetics and biodistribution in multiple organs. PLoS One 2012;7:e30491. https://doi.org/10.1371/journal.pone.0030491.

[116] Cash KJ, Li C, Xia J, Wang LV, Clark HA. Optical drug monitoring: photoacoustic imaging of nanosensors to monitor therapeutic lithium in vivo. ACS Nano 2015;9: 1692–8. https://doi.org/10.1021/nn5064858.

[117] Lee CH, Folz J, Zhang W, Jo J, Tan JWY, Wang X, et al. Ion-selective nanosensor for photoacoustic and fluorescence imaging of potassium. Anal Chem 2017;89: 7943–9. https://doi.org/10.1021/acs.analchem.7b00930.

[118] Tan JWY, Lee CH, Kopelman R, Wang X. Transient triplet differential (TTD) method for background free photoacoustic imaging. Sci Rep 2018;8:9290. https://doi.org/10.1038/s41598-018-27578-9.

[119] Zhang C, Zhang YS, Yao D-K, Xia Y, Wang LV. Label-free photoacoustic microscopy of cytochromes. J Biomed Opt 2013;18:20504. https://doi.org/10.1117/1.JBO.18.2.020504.